Long-term modification of cortical synapses improves sensory perception

Published in final edited form as:
Nat Neurosci. 2013 January ; 16(1): 79–88. doi:10.1038/nn.3274.

Long-term modification of cortical synapses improves sensory perception

Robert C. Froemke[1,2,3,*], **Ioana Carcea**[1,2,*], **Alison J. Barker**[3], **Kexin Yuan**[3], **Bryan Seybold**[3], **Ana Raquel O. Martins**[1,2,4], **Natalya Zaika**[1,2], **Hannah Bernstein**[1,2], **Megan Wachs**[5], **Philip A. Levis**[5], **Daniel B. Polley**[6], **Michael M. Merzenich**[3], and **Christoph E. Schreiner**[3]

[1]Molecular Neurobiology Program, The Helen and Martin Kimmel Center for Biology and Medicine at the Skirball Institute for Biomolecular Medicine, Departments of Otolaryngology, Physiology and Neuroscience, New York University School of Medicine, New York, New York, USA

[2]Center for Neural Science, New York University, New York, New York, USA

[3]Coleman Memorial Laboratory and W.M. Keck Foundation Center for Integrative Neuroscience, Neuroscience Graduate Group, Department of Otolaryngology, University of California, San Francisco, California, USA

[4]PhD Programme in Experimental Biology and Biomedicine, Center for Neurosciences and Cell Biology, University of Coimbra, Portugal

[5]Computer Systems Laboratory, Departments of Electrical Engineering and Computer Science, Stanford University, Palo Alto, California, USA

[6]Eaton-Peabody Laboratory, Massachusetts Eye and Ear Infirmary, Department of Otology and Laryngology, Harvard Medical School, Boston Massachusetts, USA

Abstract

Synapses and receptive fields of the cerebral cortex are plastic. However, changes to specific inputs must be coordinated within neural networks to ensure that excitability and feature selectivity are appropriately configured for perception of the sensory environment. Long-lasting enhancements and decrements to rat primary auditory cortical excitatory synaptic strength were induced by pairing acoustic stimuli with activation of the nucleus basalis neuromodulatory system. Here we report that these synaptic modifications were approximately balanced across individual receptive fields, conserving mean excitation while reducing overall response variability. Decreased response variability should increase detection and recognition of near-threshold or previously imperceptible stimuli, as we found in behaving animals. Thus, modification of cortical inputs leads to wide-scale synaptic changes, which are related to improved sensory perception and enhanced behavioral performance.

Correspondence : Robert C. Froemke Phone: 212-263-4082 robert.froemke@med.nyu.edu.
*These authors contributed equally to this work.

Competing interests statement: The authors declare that they have no competing financial interests.

Author contributions R.C.F., I.C., D.B.P., M.M.M., and C.E.S. designed the experiments. R.C.F., I.C., and A.R.O.M. performed the electrophysiological experiments. R.C.F., I.C., A.J.B., K.Y., B.S., N.Z., and H.B. performed the behavioral experiments. M.W. and P.A.L. designed and built the wireless device. R.C.F. wrote the manuscript, all authors discussed the manuscript.

Introduction

Receptive fields of sensory cortical neurons are highly structured. The anatomical arrangement and strength of synaptic inputs contributes to the functional organization of receptive fields, which in turn underlie the perception of the external world[1-4]. Cortical receptive fields are plastic, meaning that the feature selectivity of individual neurons and cell assemblies can be modified in a manner that depends on the patterns of electrical activity[5-8], sensory experience[9-18], and engagement of neuromodulatory systems such as the cholinergic nucleus basalis[19-24]. Furthermore, various forms of behavioral conditioning and learning are often, but not always, correlated with changes in cortical organization, synaptic strength, and response properties. Receptive field plasticity allows cortical neurons to act as dynamic filters, adjusting tuning curves and response properties depending on novelty or behavioral significance of certain inputs[25,26]. These changes are believed to be adaptive, in that they may underlie perceptual learning, facilitating the identification and discrimination of relevant environmental features and sensory objects. However, there is currently little experimental evidence in support of this hypothesis[27,28]. Behavioral training can improve some perceptual abilities without obvious changes in cortical responses[24,29], and studies that have directly examined cortical receptive field plasticity in a behavioral context have variously found enhancements[24,30,31], reductions[32], or no corresponding effect on perceptual abilities[6,30].

Given the precision of receptive field organization in the mature nervous system, persistent modifications of synaptic strength *in vivo* must be carefully orchestrated and coordinated within the overall cortical network, in order to emphasize certain features while preserving the relative structure and selectivity of cortical tuning. These changes are often studied in the context of behavioral conditioning or repetitive exposure to sensory stimuli. In these cases, specific responses to paired or exposed stimuli are generally enhanced[13-18]. One of the main mechanisms thought to underlie this enhancement is long-term potentiation (LTP) of intracortical excitatory inputs[7,8,17,22]. However, theoretical studies have shown that forms of competitive synaptic modifications such as LTP or long-term depression (LTD) are, by themselves, destabilizing influences on network activity. LTP and LTD are positive feedback processes that drive neural networks into hyper- or hypo-excitable states, respectively, and seem to be insufficient for behaviorally-meaningful memory storage[33,34]. While various activity-dependent and independent mechanisms have been proposed to counteract these problems and help normalize receptive fields - including homeostatic control of neurotransmitter receptor and ion channel expression[35], heterosynaptic plasticity[36], anti-Hebbian plasticity[37], and metaplastic modification of synaptic learning rules[11] - it is as of yet unknown how the synaptic drive onto cortical neurons is monitored and calibrated in the intact brain, to allow changes in sensory representation to positively influence perception and behavior.

Results

Synaptic modifications conserve net excitation

We investigated the coordination of synaptic receptive field plasticity across multiple inputs and stimulus parameters by making whole-cell recordings from 29 neurons of adult rat primary auditory cortex (AI) *in vivo*[17,20,23,38]. To rapidly and reliably reorganize synaptic receptive fields of AI neurons, recordings were combined with electrical stimulation of the cholinergic nucleus basalis[20-24] (Fig. 1a), mimicking the activation of this neuromodulatory system during directed attention or arousing behavioral episodes[39,40]. Excitatory synaptic receptive fields were measured in voltage-clamp by playing pseudo-random sequences of pure tones, varying in intensity from 10-80 dB sound pressure level (SPL) and frequency from 0.5-32 kHz. After characterizing baseline responses for 5–15 minutes, modifications of

AI synaptic receptive fields were induced by repetitively pairing nucleus basalis stimulation with a tone of specific intensity and frequency for 1–5 minutes ('nucleus basalis pairing'), using optimized parameters for pairing first identified with extracellular recordings (Supplementary Fig. 1) and confirmed with intracellular recordings (Supplementary Fig. 2). After pairing ended, receptive fields were monitored for the duration of stable recordings (see **Methods**).

We found that nucleus basalis pairing induced a set of highly organized changes across the entire frequency-intensity synaptic receptive field (Fig. 1b,c; Supplementary Fig. 3). In particular, increases in excitation at the paired inputs were matched closely by corresponding decreases at the original best stimuli (which initially evoked the largest response), leading to a conservation of excitatory input received by AI neurons.

In the example recording shown in Figure 1, 4 kHz tones of 30 dB SPL intensity were paired with nucleus basalis stimulation for three minutes. Before pairing, the peak intensity level was 80 dB SPL and the best frequency was 16 kHz. After pairing, excitation increased dramatically at the paired stimulus (Fig. 1b,c). Additionally, while only 30 dB SPL, 4 kHz tones were presented during nucleus basalis stimulation, excitation at the original best stimulus decreased (80 dB SPL, 16 kHz; Fig. 1b,c; for three other examples, see Supplementary Fig. 3). While changes to some individual unpaired tones could be observed, responses to unpaired stimuli on average were not significantly different after pairing. The net result of these modifications was to shift the preferred sound level and frequency tuning of this neuron while preserving the total strength of excitatory input across all stimuli (Fig. 1c).

For 29 recordings, these long-term changes in synaptic strength were on average specific to particular stimuli across dimensions of both intensity (Fig. 2a) and frequency (Fig. 2b). For intensity sensitivity, maximum enhancements were observed at the paired level, although increases often spread to lower intensities as well (Fig. 2a, **top**; Supplementary Figs. 2a,b). Increased excitation at paired stimuli were matched by decreased excitation at original preferred stimuli (Figs. 2a,b, **bottom**), albeit with a somewhat slower time course (~10–20 minutes; Fig. 2c). These pairing-induced changes to synaptic strength cooperated to shift intensity sensitivity profiles of AI neurons, making them more non-monotonic with regard to sound level (Supplementary Fig. 4), and conserved the net excitatory drive received by AI neurons, such that the relative magnitudes of individual enhancements were approximately balanced by an equivalent amount of reduction (Fig. 2d).

These changes seemed to be specific to cortical neurons, as indicated by three sets of experiments. First, we made seven multiunit recordings from the ventral division of the medial geniculate body (MGB), the main auditory thalamus. We did not observe long-term changes of MGB responses after nucleus basalis pairing (Supplementary Figs. 1c,d), suggesting that thalamic spiking output is not persistently affected by pairing. However, under different conditions, it is possible that thalamic responses are modified, and it remains possible that pairing can induce plasticity in other parts of the MGB such as the medial division.

Second, long-term changes in tone-evoked inhibitory responses of AI neurons were also induced by pairing (Supplementary Fig. 5a,c), such that inhibitory responses at the paired stimulus and original best stimulus were reduced. In particular, in the example shown in Supplementary Figure 5a, reductions in tone-evoked inhibition were observed at both the paired (circle) and original best frequency (square). Over the population of 29 recordings, however, inhibition at the paired input began to recover (Supplementary Fig. 5c), and as previously reported, eventually recovered to match and re-balance the strength of

excitation[22]. As inhibitory inputs to AI neurons are intracortical, this provides additional evidence, together with local microstimulation experiments of thalamic and intracortical inputs[22], for a cortical locus of synaptic modification.

Third, we found that topical AI application of cholinergic or NMDA receptor antagonists prevented modifications of excitatory and inhibitory tuning curves by nucleus basalis pairing. Application of the muscarinic receptor antagonist atropine (1 mM; Supplementary Fig. 6a) blocked short- and long-term changes, suggesting that despite GABAergic and peptidergic projections from nucleus basalis[41,42], muscarinic receptor activation is required for both the immediate and enduring effects of nucleus basalis pairing. Example excitatory and inhibitory tuning curves from the same neuron are shown in Supplementary Figure 6a, top (excitation) and middle (inhibition), before and 10 minutes after pairing; results from five experiments are summarized in Supplementary Figure 6a, bottom. Similarly, cortical application of the NMDA receptor blocker AP5 (1 mM; Supplementary Fig. 6b) also prevented long-term (but not the immediate) effects of pairing on excitation and inhibition in six neurons, demonstrating that excitatory and inhibitory modifications are consolidated downstream of NMDA receptor activation.

Therefore, similar to frequency tuning[21,22], the peak sound levels and overall intensity sensitivity profiles of AI synaptic responses are plastic and can be regulated conjointly. These changes act together to locally enhance paired stimuli while globally normalizing excitability across frequency-intensity synaptic receptive fields. Such synaptic modifications are longer-term consequences of complex processes engaged by neuromodulation and nucleus basalis pairing, similar to what might hypothetically occur during episodes of directed attention to salient or behaviorally-meaningful stimuli[39-42]. It is important to note, however, that selective attention might engage additional mechanisms also important for processing sensory information, such as decorrelating activity patterns across different neurons or cell assemblies[23,40,43-45].

Best stimuli are dynamically determined

How are neurons or local networks able to sense and selectively modify responses to their original preferred or best stimuli? Previous studies of cortical receptive field plasticity in the visual system have examined the role that homeostatic modifications of synaptic transmission and excitability play in receptive field remodeling, especially after prolonged periods of monocular deprivation[11,33,35]. However, here, such homeostatic mechanisms may be too protracted and non-specific to account for the reduction at the original best stimulus, which decreases over 10–20 minutes. Given that the best stimulus itself is an empirically-determined local maximum, we next asked if this suppression of synaptic strength was an activity-dependent process sensitive to the recent stimulus history.

To assess to what degree the reduction of synaptic strength at the original best stimulus was experience dependent, we played a restricted stimulus set (generally 10–60 dB SPL tones at 0.5–32 kHz) for approximately 10 minutes after pairing, excluding the original best stimulus (usually at 70–80 dB SPL). Afterward, we then played the full stimulus set for the remainder of the recording, in order to re-characterize the synaptic receptive field and determine whether post-pairing presentation of the original best stimulus was necessary for the observed reduction in excitation evoked by those tones.

The absolute best stimulus for one example recording was an 80 dB SPL, 1 kHz pure tone, with strong responses to nearby, ‘relative best stimuli’ of 1–2 kHz at 60–80 dB SPL (excitatory responses for this cell are shown in Figure 3a; inhibitory responses in Supplementary Figure 5b). Tones of 30 dB SPL, 4 kHz were used during pairing for this recording. After pairing, only stimuli 10-60 dB SPL were played for 10 minutes (thus

excluding absolute best stimuli). We then resumed measuring the frequency-intensity synaptic receptive field with the full stimulus set, and found that, while excitatory responses to the paired tone had increased (Fig. 3a, circles), excitatory responses to the original absolute best stimulus were unchanged (Fig. 3a, squares). However, analysis of post-pairing changes throughout the synaptic receptive field revealed reductions to relative best stimuli that were included in the restricted stimulus set. Responses to 60 dB SPL, 2 kHz tones (the 'relative best stimulus', i.e., whichever stimulus of <70 dB SPL that evoked the largest pre-pairing responses), were depressed 10-20 minutes after pairing (Fig. 3a, diamonds).

The reduction of responses at the absolute best or relative best stimuli ('best stimuli depression') thus seemed to require presentation of those tones in a prolonged period after the pairing procedure. For 13 recordings, responses evoked by relative best stimuli at lower intensity levels (usually at 60 dB SPL) were consistently reduced when included in the restricted stimulus set (excitation: Fig. 3b, left; inhibition: Supplementary Fig. 5d), while original absolute best stimuli at higher intensity levels were unchanged when those stimuli were not presented. These results indicate that the best stimulus of a neuron is dynamically determined following periods of receptive field reorganization, likely requiring several minutes of stimulus presentation to assess the statistics of sensory input.

This regulatory process of best stimuli depression could require a certain duration (e.g., approximately 10 minutes) to elapse, regardless of the amount of stimulus iterations. Alternatively, best stimuli depression could require a certain number of tones to be presented, independent of duration. To resolve this issue, we varied the intervals between pure tone presentation after pairing, playing stimuli either at a slower rate (~1/20 seconds, i.e., 0.05 Hz), a moderate rate (~1/10 seconds, 0.1 Hz), or a faster rate (~1/2 seconds, 0.5 Hz). We then monitored the change in response at best stimuli at two different times: after 11-20 stimulus presentations or after 51-60 stimulus presentations. If best stimuli depression was strictly time-dependent, then we hypothesized that after 60 presentations, responses should be progressively more depressed from faster to slower presentation rates, as more time would have elapsed over the slower rate. Conversely, if best stimuli depression was accretive, then similar amounts of depression should be observed after 60 presentations irrespective of rate over this range.

We found that the magnitude of best stimuli depression was equivalent after 51–60 stimulus presentations regardless of rate (Fig. 3b, **right**), but not after 11–20 presentations in any of the three cases. These results demonstrate that 20–60 presentations of these tones are required for best stimuli depression, at least when presented within ~1–20 minutes. Furthermore, these data strengthen the hypothesis that best stimuli depression, and the resulting normalization of net excitation onto AI neurons after pairing, is input specific and activity dependent. Thus, while mature AI receptive fields are usually quite stable[46], events such as nucleus basalis pairing transiently destabilize cortical tuning by enhancing responses to paired, possibly behaviorally-relevant stimuli. To compensate for such changes in excitation, stimulus history appears to be monitored for minutes to hours afterward, allowing cortical networks to preserve excitability and receptive field structure by reducing the empirically-determined largest evoked responses among the unpaired stimuli. Furthermore, paired stimuli themselves may be protected from this depression.

Reduced variability improves signal processing

Long-term changes in cortical synaptic receptive field organization might have important consequences for information processing and perception of sensory stimuli. In the remainder of this study, we used three different methods to evaluate changes in cortical function and signal processing after pairing: analytical (computing mutual information and variability of

synaptic responses), electrophysiological (examining spiking receptive fields), and psychophysical (performing nucleus basalis pairing in behaving animals).

Two main tasks that sensory systems must accomplish are signal detection and recognition[47,48]. These functions can be challenging even in relatively quiet, controlled environments, because in cortical circuits, sensory-evoked excitatory responses occur within a noisy background of spontaneous activity (Fig. 4a, **top**), with variable single-trial amplitudes close in size to those triggered by other stimuli (Fig. 4b, **top**). We noticed that, particularly after pairing nucleus basalis stimulation with low intensity tones, the magnitude of initially-small responses to paired stimuli increased in parallel with decreases of the largest responses (Fig. 1b, **top**). This observation suggested that while the mean EPSC size over all stimuli remained unchanged, the total variance of AI synaptic tuning curves and receptive fields may be reduced.

Detection of sensory input requires that tone-evoked events can be reliably resolved from spontaneously-occurring synaptic events. At the same time, cortical representations of sensory percepts must be statistically distinct for correct recognition of stimuli and discrimination between different inputs. To examine whether changes to signal detection and recognition capacities might be represented at the level of synaptic inputs to AI, and therefore could be maintained for minutes to hours after pairing, we quantified changes to distributions of tone-evoked ('signal') and spontaneous ('noise') EPSCs over frequency-intensity receptive fields. After measuring these distributions before and after pairing, we computed two different metrics: an index of variability q, the variance of synaptic amplitudes normalized by mean amplitude[38], and the mutual information between the signal and noise distributions[48]. In this context, mutual information is related to the probability that at any time, a given synaptic response was either stimulus evoked or occurred spontaneously.

We found that nucleus basalis pairing increased mutual information and decreased q. Distributions of tone-evoked and spontaneous EPSCs for the recording in Figure 1 are shown in Figure 4a, **bottom**. Before pairing, there was considerable overlap between these distributions (Fig. 4a, **bottom left**). After pairing low-intensity tones with nucleus basalis stimulation, the distribution of spontaneous activity was essentially unchanged, while the standard deviation of the tone-evoked response distribution subtly but significantly decreased, although mean amplitude was conserved (Fig. 4a, **bottom right**). As a result, the mutual information for signals increased, i.e., the uncertainty about the presence of a signal in the noise was reduced as there was less overlap between signal and noise distributions. While these effects may be modest in individual recordings, small gains in single cells may have substantial effects at the population level. This suggests that quiet sounds would become easier to detect. Over 29 recordings, mutual information between signal and noise distributions increased (Fig. 4c, **top left**; Supplementary Figure 7a) and q decreased (Fig. 4c, **top right**), due to reductions of standard deviations (Fig. 4c, **bottom right**) with little change in mean amplitudes (Fig. 4c, **bottom left**). In 22/29 recordings, signal distributions became more statistically distinct from noise distributions after pairing (measured with Student's paired two-tailed t-tests). In 5 cases, signal distributions were initially statistically similar to noise distributions ($p>0.05$) but became significantly different ($p<0.05$) after pairing.

Similar analyses indicated that recognition of paired from unpaired stimuli would also be enhanced by pairing, although by a complementary mechanism: increase in distribution mean (Fig. 4b, **bottom**). Before pairing, responses to tones chosen for pairing were approximately the same as responses to most other tones. After pairing, responses that were initially weak became stronger, increasing mutual information conveyed by paired versus

non-paired tones (Fig. 4d, **top left**; Supplementary Figure 7b). Pairing also decreased *q* for responses to paired inputs (Fig. 4d, **top right**), by increasing mean amplitude (Fig. 4d, **bottom left**) while standard deviations were not significantly affected (Fig. 4d, **bottom right**). As the sizes of paired distributions could be much smaller than the unpaired distributions, we cross-validated this analysis using t-tests. We found that 17/29 recordings showed lower p-values between paired and unpaired distributions after pairing (10/29 cases changing from statistically similar to statistically distinct), and 16/29 recordings showed lower p-values between paired and noise distributions after pairing (7 recordings changing from statistically similar to statistically distinct at the $p<0.05$ level).

Synaptic modifications affect spike output

To be useful for improving perceptual abilities in behaving animals, alterations in cortical receptive fields and signal processing at the level of synaptic inputs should also be represented by changes to spiking receptive fields. To determine whether pairing improved information processing at the level of action potential generation, we made current-clamp recordings from AI neurons *in vivo* and measured tone-evoked suprathreshold responses.

For intensity sensitivity (Fig. 5a) and frequency tuning (Fig. 5b), pairing enhanced spike counts evoked by paired tones and reduced spiking evoked by original best stimuli. As with synaptic strength, the net effect of these adjustments was that the total number of evoked spikes over all presented stimuli was kept constant (Fig. 5c), and mutual information for both signal detection and recognition increased (Fig. 5d).

Synaptic modifications improve perception

Attention and arousal facilitate sensory processing, and the nucleus basalis neuromodulatory system is critically linked to activation of attentive behavioral states[25,40]. Our analyses of synaptic distributions (Fig. 4) and measurements of spiking tuning curves (Fig. 5) both indicated that the changes to excitatory receptive fields induced by a few minutes of nucleus basalis pairing should improve auditory perception, particularly for subliminal stimuli with initially weak, subthreshold responses. Therefore, in our final experiments, we examined the psychophysical abilities of adult animals to perceive specific tonal stimuli (‘targets’), focusing on two separate aspects of sensory perception: detection of target stimuli over a range of intensities, and recognition of target stimuli from non-target tones (‘foils’).

Rats were operantly conditioned to nose-poke for a food reward in response to target stimuli (4 kHz tones, any intensity), while withholding responses to foil tones of other frequencies. Animals had stimulation electrodes implanted into right nucleus basalis, and cannulas for drug delivery implanted unilaterally into ipsilateral AI. After two weeks of training, animals reached plateau levels of performance for relatively loud, salient target stimuli.

The psychophysical detection abilities of one representative animal is shown in Figure 6a, and the performance of all animals are individually shown in Supplementary Figure 8 and summarized in Figures 6c-e. Animals achieved high hit rates for targets (Fig. 6a, black circles) and a low number of false alarm responses to foils (Fig. 6a, black triangles). Consequentially, d’ values were quite good for louder tones considerably above perceptual threshold, while tones below ~50 dB SPL were detected less reliably.

After determining response rates and d’, we repetitively paired 4 kHz tones at a single lower intensity (between 30–45 dB SPL) with nucleus basalis stimulation for 3–5 minutes while animals were awake in the training box. We then re-tested their perceptual abilities to detect 4 kHz tones. At the paired stimulus intensity, detection was much higher, with average d’ more than doubling 30–120 minutes after pairing (Fig. 6c and e, red squares). This was due

to an increase in hit rate at the paired intensity (Fig. 6a and d, red circles), with no significant change in false alarms (Fig. 6a and d, red triangles). Data shown are averaged over two days of training; as shown in Figure 6f, baseline daily performance of individual animals was approximately the same at the start of the first day and the second day. Thus pairing nucleus basalis activation with presentation of low intensity sounds makes it easier for animals to perceive and operate on these initially hard-to-hear stimuli, perhaps by a selective reduction in thresholds for spike generation and/or perception.

Changes to AI networks could lead to substantial perceptual improvements in initially-trained animals. We found that, instead of nucleus basalis stimulation, pairing low intensity tones with direct AI infusion of the cholinergic agonist carbachol (1 mM) also was effective at increasing detection of the paired tone (Fig. 6b,c, open squares). This demonstrated that changes localized or initiated directly within AI could enhance auditory perception, after the basic audiomotor association for the task had been formed. As a control, saline infusion paired with low intensity tones had no effect (Fig. 8c, open diamonds). In contrast, increased detection abilities after nucleus basalis pairing were prevented when either the muscarinic receptor antagonist atropine (1 mM, Fig. 6g,i, filled diamonds) or the NMDA receptor blocker AP5 (1 mM, Fig. 6h,i, open diamonds) were infused into AI, indicating that long-term modification of AI synapses is required for enhanced tone detection.

We further tested whether pairing in awake animals would improve recognition abilities. Initially, foil stimuli were spectrally dissimilar from the target stimulus of 4 kHz, separated at one octave intervals at 70 dB SPL. Animals could easily respond to targets and withhold responses to foils on this ‘wideband’ task before pairing, as shown for one example animal (Fig. 7a, black dashed line), and for all 12 animals tested on this task (Fig. 7d). Unsurprisingly, pairing with 4 kHz tones failed to improve recognition (example animal: Fig. 7a, red solid line; all animals: Figs. 7c,d,f), as animals were already performing close to optimum.

We then made this task more challenging, by compressing the spectral range of the foils from six octaves to one octave, such that the foils were much more similar to the target tone. Before pairing, behavioral performance on this ‘narrowband’ task was low (example animal: Fig. 7b, black dashed line; all animals: Figs. 7c,e,f), but pairing greatly improved frequency recognition (example animal: Fig. 7b, red solid line; all animals: Figs. 7c,e,f). This increase in performance was prevented by administration of atropine, either directly into AI via cannula (Figs. 7g,i, filled diamonds) or given systemically (Fig. 7i, open diamonds).

Overall, 7/9 animals showed a significantly higher hit rate ($p<0.05$, Student’s paired two-tailed t-test) in the detection of the target tone at the paired intensity after pairing (Supplementary Fig. 8). On the narrowband recognition task, 7/12 animals showed a significantly higher hit rate on the target frequency after pairing (Supplementary Fig. 9), while only 1/12 animals improved performance on the wideband recognition task (Supplementary Fig. 10).

We then tested if changes to paired inputs alone could enhance perceptual abilities; alternatively, perhaps best stimuli depression and corresponding changes in full synaptic receptive field variance are required for improved sensory perception. In behaving animals, we found that nucleus basalis pairing enhanced recognition on the narrowband task for tones at 70 dB SPL only when the full stimulus set was played after pairing. If instead, a reduced set of targets and foils was presented for 30 minutes afterward that did not contain any tones over 50 dB SPL, pairing failed to improve target recognition at higher intensity levels (example animal: Fig. 7h; all animals: Fig. 7i, triangles). Therefore, although nucleus basalis pairing induces enhancements in responses to paired stimuli, wide-scale receptive field

reorganization mediated by large range stimulus exposure- leading to decreased response variability- is required for these changes to be perceptually useful. Given the relatively rapid gains in performance, our results indicate that best stimulus depression is required for cortical receptive field reorganization to have functional significance. Without it, perceptual improvement is limited and the benefits of cortical plasticity may be compromised.

Lastly, although these behavioral changes were observed when nucleus basalis pairing was performed in awake animals, the electrophysiological data were obtained in anesthetized animals. To more closely connect the physiological and behavioral effects of pairing, we conducted additional behavioral experiments, performing pairing in animals that were temporarily anesthetized. Baseline behavioral performance of trained, implanted animals was monitored for 30–60 minutes. Animals were then anesthetized either with pentobarbital ('Pento'; Figs. 8a-d) or isoflurane ('Iso', 3-5%; Figs. 8e-h), and five minutes of pairing with 4 kHz tones was performed. Animals were allowed to recover (usually after 1–2 hours for isoflurane or 3–5 hours for pentobarbital), and post-pairing behavioral performance assessed for 1–2 hours. As shown in Figure 8, significant improvements on the detection and narrowband recognition tasks were observed even when pairing was performed in animals that were anesthetized during pairing. Thus the changes in neural circuits initiated by nucleus basalis pairing persist and can affect behavioral performance even after major changes in brain state.

Discussion

The central nervous system remains plastic throughout life, adapting to behaviorally-relevant changes in the external environment. Previous studies have documented the alterations to cortical circuits and elsewhere within the brain that are correlated with periods of behavioral training and conditioning[10,49]. Here we used a different approach to assess the causal value of such modifications to cortical synaptic receptive fields, taking advantage of the powerful neuromodulatory system of the cholinergic nucleus basalis to mimic the neural processes engaged by and important for attention. Nucleus basalis pairing modifies intracortical synapses in absence of changes to thalamocortical transmission[22], allowing us to selectively probe the behavioral and network effects of direct changes to cortical synapses and receptive fields.

Our data demonstrate how excitatory inputs to the cerebral cortex are coordinated *in vivo* to accommodate changes in sensory representations for perceptual learning. Multiple parameters of AI receptive fields are rapidly changed by pairing a specific input with nucleus basalis activation. In particular, neurons that initially prefer higher-intensity tones can be re-tuned to prefer lower-intensity stimuli. Synaptic enhancements at paired inputs are coupled with reductions in responses to previously-strong inputs, in a manner that depends on the statistics of the acoustic environment experienced immediately following each episode of nucleus basalis pairing. We predict that these changes serve to transiently increase the similarity between cortical neurons by enhancing responses to the shared, paired input and decreasing responses to originally preferred (possibly distinct) inputs. As a consequence of having more similar receptive fields, we speculate that stimulus and noise correlations between neuronal firing patterns may be higher, possibly improving signal processing and information transmission to downstream stations. Further experiments will be necessary to clarify this issue of the effects of synaptic plasticity and attentional modulation on cortical correlation[23, 43-45].

Our experiments indicate that, in addition to the tone presented during nucleus basalis stimulation, the statistics of the post-pairing acoustic environment also play a major role in determining how AI synapses and tuning curves are adjusted after pairing. In particular, it

seems that cells and networks are able to compute their local maximal best stimulus, to reduce those responses and compensate for the increase of excitation at the paired input. The integrative time for this process seemed to be at least 10 minutes, and future studies are required to determine the duration of this 'sensitive period' for best stimulus depression, the cellular mechanisms and relation to phenomena such as heterosynaptic LTD, and the perceptual impact of changes to input statistics. Importantly, a recent study of acoustic perceptual learning in human subjects demonstrated that passive stimuli presented during the post-training period could also influence the degree of learning[50]. However, stimuli presented more than 15 minutes after a period of practice were less effective, and stimuli presented four or more hours after practice were found to be ineffective.

Functionally, changes to AI synapses alone are presumably insufficient to generate behavioral modification in untrained animals, which require extensive training on the procedural aspects of the tasks. However, once the initial audiomotor associations have been formed, modifications of AI circuitry can lead to superior behavioral performance for recognizing paired tones from spectrally-similar unpaired tones, and enhance the perception of liminal, low-intensity stimuli.

Methods

Surgical preparation

All procedures were approved under NYU and UCSF IACUC protocols. Experiments were carried out in a sound-attenuating chamber. Female Sprague-Dawley rats 3-5 months old were anesthetized with pentobarbital. A bipolar stimulation electrode was implanted in the right nucleus basalis (stereotaxic coordinates from bregma, in mm: 2.3 posterior, 3.3 lateral, 7 ventral) and the right auditory cortex was exposed. Pure tones (10-80 dB SPL, 0.5-32 kHz, 50 msec, 3 msec cosine on/off ramps) were delivered in pseudo-random sequence. AI location was determined by mapping multiunit responses 500-700 μm below the surface using tungsten electrodes[15,22].

Whole-cell recording

In vivo whole-cell recordings were obtained from neurons located 400-1100 μm below the pial surface. Recordings were made with an AxoClamp 2B (Molecular Devices). For voltage-clamp, patch pipettes (5-9 MΩ) contained (in mM): 125 Cs-gluconate, 5 TEACl, 4 MgATP, 0.3 GTP, 10 phosphocreatine, 10 HEPES, 0.5 EGTA, 3.5 QX-314, 2 CsCl, pH 7.2. For current-clamp, pipettes contained: 135 K-gluconate, 5 NaCl, 5 MgATP, 0.3 GTP, 10 phosphocreatine, 10 HEPES, 0.5 EGTA, pH 7.3. Resting potential: −65.2±9 mV (s.d.); series resistance (R_s): 25.0±6 MΩ; input resistance (R_i): 108.1±58 MΩ. Data were excluded if R_i or R_s changed >30% from values measured during baseline. Data were filtered at 2 kHz, digitized at 10 kHz, and analyzed with Clampfit 10 (Molecular Devices). After recording baseline responses for each cell, a non-preferred tone of a given intensity level and frequency was repetitively presented (1-5 min) during nucleus basalis stimulation (250 msec, 100 Hz). Tone onset occurred 20 or 100 msec after the start of nucleus basalis stimulation. In voltage-clamp, we measured peak excitatory current amplitudes at −70 mV and peak inhibitory current amplitudes at either −20 mV or 0 mV. Other aspects of some recordings (15/29 experiments in Fig. 2) were previously analyzed in terms of the changes to excitatory and inhibitory frequency tuning for a prior study[22].

Behavior

Rats were lightly food-deprived and pre-trained for 1-4 weeks on a frequency recognition go/no-go task. Animals were rewarded with food for nosepoking within three seconds of presentation of a target tone (4 kHz, any intensity), and given a short (~5 s) time out if they

incorrectly responded to non-target tones. After learning to nosepoke to 4 kHz tones, spectrally-wideband foils were also presented (0.5, 1, 2, 8, 16, 32 kHz). Animals that achieved hit rates >66.6% for targets were then anesthetized with ketamine/xylazine, had stimulation electrodes chronically implanted in right nucleus basalis, cannulas implanted into right AI, and allowed to recover for a week. Each implanted animal was first tested on the 'wideband' recognition task or the detection task for at least 1-2 days. On the wideband task, tones (target: 4 kHz; foils: 0.5, 1, 2, 8, 16, 32 kHz) were presented at 70 dB SPL. On the detection task, tones were presented at 20-90 dB SPL. On each day, tones were presented for 30-60 minutes to assess baseline performance; 4 kHz tones (at 70 dB SPL for the wideband recognition task; 30-45 dB SPL for the detection task; hits binned over 20-45 dB SPL) were then paired with nucleus basalis stimulation in the training box for three to five minutes, and behavior assessed and quantified 30-120 minutes afterward. Animals were then randomly assigned to be part of an experimental group: detection in which pairing was combined with infusion of saline, atropine, or AP5 into the AI cannula (0.4-1.0 μL, 1 mM), or narrowband recognition (foils: 2.8, 3.2, 3.6, 4.5, 5.1, 5.7 kHz at 70 dB SPL) in which pairing was combined with infusion of saline or atropine, or pairing was followed by 30 minutes of low-intensity tone presentation ('quiet' stimuli of <50 dB SPL over the same range of frequencies). Choice of experimental group was made regardless of baseline performance on these tasks, which were statistically similar across groups; for detection: nucleus basalis pairing mean pre d' was 0.7±0.2 and mean pre hit rate was 47.7±4.6%, carbachol pairing mean pre d' was 1.0±0.5 ($p>0.5$ compared to nucleus basalis paired animals, Student's unpaired two-tailed t-test) and mean pre hit rate was 58.0±7.3% ($p>0.2$ compared to paired animals), atropine mean pre d' was 0.7±0.4 ($p>0.9$) and mean pre hit rate was 36.8±5.5% ($p>0.1$), AP5 mean pre d' was 0.9±0.2 ($p>0.4$) and mean pre hit rate was 60.1±8.4% ($p>0.1$); for narrowband discrimination: nucleus basalis pairing mean pre d' was 0.5±0.1 and mean pre hit rate was 50.1±6.6%, atropine mean pre d' was 0.9±0.4 ($p>0.1$) and mean pre hit rate was 55.7±7.0% ($p>0.6$), 30′ quiet mean pre d' was 0.8±0.2 ($p>0.05$) and mean pre hit rate was 66.2±9.8% ($p>0.1$). For animals exposed to quiet stimuli, responses to 4 kHz target stimuli were still rewarded. Five animals received atropine systemically (1 mM, 2 mg/kg; Fig. 7i, open diamonds) and five animals through a cannula implanted in AI (filled diamonds). For stimulation, three animals wore a miniature custom-built high-amplitude current generator on a backpack, to allow them to move freely around the training box. This device utilizes MICAz wireless sensing devices ('motes') running the TinyOS operating system for on-line stimulator control, and consists of two parts: the 'rat mote,' worn by the animal in a backpack, and the 'base mote,' placed in the cage. Performances of the three animals who used the backpack-mounted stimulator were similar to the other animals who were tethered to the current generator for the wideband task ($p>0.2$).

Statistical analysis

For electrophysiological recordings, Student's paired two-tailed t-test was used for comparison unless otherwise noted. Power analysis was performed to determine the number of cells required for statistical significance. For whole-cell recordings, effect size was 1.40 and power was 0.82, requiring a sample size of at least five neurons (which is satisfied in all electrophysiological experiments summarized in Figures 2-5, and Supplementary Figures 2 and 6). For multiunit recordings, effect size was 0.94 and power was 0.82, requiring at least nine recordings, satisfied in Supplementary Figure 1.

Threshold of synaptic receptive fields (light-blue lines in Figures 1c, 3a, and Supplementary Figs. 3, 5) were assessed by measuring the distribution of baseline current noise for each cell (mean trial-by-trial noise level generally <5 pA). We then compared the noise distribution to the distribution of tone-evoked events for each stimulus; threshold was then defined where

the tone-evoked peak currents were significantly larger than noise ($p<0.05$). As paired intensities (30-80 dB SPL) tended to be substantially higher than these thresholds (10-40 dB SPL), nucleus basalis pairing had no significant effect on minimum synaptic response threshold (two neurons increased threshold by 10 dB SPL, two neurons decreased threshold by 10 dB SPL, $p>0.5$).

To compute the degree of conservation of excitation (in Figure 2d), for each cell, we subtracted the baseline response from the post-pairing response for each stimulus. We then normalized these differences by the mean baseline response (over the entire frequency-intensity receptive field, across the paired frequency axis, or across the paired intensity axis), and separately summed the positive values (for increases in response after pairing) and negative values (for decreases). These were then tabulated for each of the 29 whole-cell voltage-clamp recordings, and the absolute values of total normalized increases and total normalized decreases compared with the Mann-Whitney test.

To compute monotonicity of intensity sensitivity profiles in Supplementary Figures 4c,d, we first determined the contribution to the decrease in correlation from the changes to three of the eight intensities ('Paired & peak', the paired intensity, the intensity −10 dB SPL lower than paired, and the intensity that evoked the largest EPSC). In this case, we assumed that after pairing, responses to all other intensities remained at their original values before pairing, and calculated the corresponding linear correlation coefficient. Then to determine the contribution of changes to all other five inputs ('Other'), we assumed that after pairing, only the responses to these other stimuli were affected, while the responses to the paired, −10 dB SPL from paired, and peak intensities remained at their initial levels, and again calculated the change in correlation.

Index of variability q was defined as the variance of all synaptic responses normalized by the mean response amplitude ($\left\langle |q=\frac{\sigma^2}{\mu}| \right\rangle$) (ref. 38). For signal detection, mutual information was defined as the difference between the synaptic entropy ($H(r) = -\sum_r P(r)^* \log_2 P(r)$) and the synaptic entropy conditioned on whether a response was spontaneous ('noise') or tone-evoked ('signal'):

$$H(r|s) = -P(s=\text{signal})^* \sum_r P(r|s=\text{signal})^* \log_2 P(r|s=\text{signal}) +$$

$$\sum_r P(r|s=\text{noise})^* \log_2 P(r|s=\text{noise})$$

Mutual information for signal recognition was calculated in a similar manner, except that the 'noise' distribution contained all unpaired tone-evoked responses as well as spontaneous responses, and the 'signal' distribution only contained responses evoked by the paired tone and tones of the same frequency but −10 dB SPL lower[48]. Spontaneous events were measured in a 100-500 msec window during silent inter-stimulus intervals, and tone-evoked events measured in a 100 msec window starting at tone onset. To compare population statistics in Figures 4c, 4d, 5d, two-tailed paired Wilcoxon signed rank tests were used. Values of mutual information, q, means, and standard deviations were not statistically different between distributions comprised of random half-sized subsets of the full distributions, for either signal/noise ($p>0.1$) or the paired/unpaired data sets ($p>0.05$).

For behavioral experiments, each animal's performance was averaged over one to two days, as detection thresholds and effects of pairing were consistent for at least the first two days of stimulation (Fig. 6f), and d' values were conventionally computed as the difference in z-

scores between hits and false positives: d' = z(hit rate) – z(false positive rate). For determining the mean performance for each group of animals (Figs. 6d, 6e, 7d, 7e), each of the individual mean performance curves (shown in Supplementary Fig. 8 for detection, Supplementary Fig. 9 for narrowband recognition, and Supplementary Fig. 10 for wideband recognition) were averaged together. Power analysis was performed to determine the number of animals required for statistical significance. For detection performance, effect size was 1.52 and power was 0.87. The required sample size was at least four animals, satisfied in the detection experiments of Figures 6 and 8. For recognition experiments, effect size was 1.32 and power was 0.80, requiring at least five animals, satisfied in the recognition experiments of Figures 7 and 8.

Error bars represent means ± s.e.m.

Supplementary Material

Refer to Web version on PubMed Central for supplementary material.

Acknowledgments

We thank L.F. Abbott, T. Babcock, M. Berry, E. Chang, Z. Chen, E. de Villers-Sidani, A.L. Dorrn, P. Dutta, A. Fairhall, S.P. Gandhi, G. Glassner, C.A. Hoeffer, K. Imaizumi, B.J. Jones, N. Kopell, R. Liu, G. Myers, P. O'Hara, J. Shih, A.Y. Tan, C.-L. Teng, and L. Wilbrecht for comments, discussions, and technical assistance. J. Pivkova created the artwork in Fig. 1a. This work was supported by NIDCD (grant DC009635 to R.C.F., grant DC009836 to D.B.P., and grant DC02260 to C.E.S.), NSF (grants 0615308 and 0627126 to P.A.L.), Intel Research (P.A.L.), DoCoMo Capital and Foundation Capital (P.A.L.), the Conte Center for Neuroscience Research at UCSF (grant MH077970 to M.M.M. and C.E.S.), Hearing Research Inc. (C.E.S.), the John C. and Edward Coleman Fund (M.M.M. and C.E.S.), and the National Academies Keck Future Initiatives (R.C.F. and P.A.L.). A.J.B. is supported by a National Science Foundation Predoctoral Fellowship. M.W. is supported by a Sequoia Capital Stanford Graduate Fellowship. I.C. is supported by an NIMH training grant. P.A.L. is a Microsoft Research New Faculty Fellow. R.C.F. is a Sloan Research Fellow.

References

1. Hubel DH, Wiesel TN. Receptive fields, binocular interaction. J. Neurophysiol. 1962; 160:106–154.
2. Hirsch JA, Martinez LM. Circuits that build visual cortical receptive fields. Trends Neurosci. 2006; 29:30–39. [PubMed: 16309753]
3. Huberman AD, Feller MB, Chapman B. Mechanisms underlying development of visual maps and receptive fields. Annu. Rev. Neurosci. 2008; 31:479–509. [PubMed: 18558864]
4. Ye CQ, Poo MM, Dan Y, Zhang XH. Synaptic mechanisms of direction selectivity in primary auditory cortex. J. Neurosci. 2010; 30:1861–1868. [PubMed: 20130195]
5. Frégnac Y, Shulz D, Thorpe S, Bienenstock E. A cellular analogue of visual cortical plasticity. Nature. 1988; 333:367–370. [PubMed: 3374571]
6. Talwar SK, Gerstein GL. Reorganization in awake rat auditory cortex by local microstimulation and its effect on frequency-discrimination behavior. J. Neurophysiol. 2001; 86:1555–1572. [PubMed: 11600620]
7. Meliza CD, Dan Y. Receptive-field modification in rat visual cortex induced by paired visual stimulation and single-cell spiking. Neuron. 2006; 49:183–189. [PubMed: 16423693]
8. Jacob V, Brasier DJ, Erchova I, Feldman D, Shulz DE. Spike timing-dependent synaptic depression in the in vivo barrel cortex of the rat. J. Neurosci. 2007; 27:1271–1284. [PubMed: 17287502]
9. Katz LC, Shatz CJ. Synaptic activity and the construction of cortical circuits. Science. 1996; 274:1133–1138. [PubMed: 8895456]
10. Buonomano DV, Merzenich MM. Cortical plasticity: from synapses to maps. Annu. Rev. Neurosci. 1998; 21:149–186. [PubMed: 9530495]
11. Smith GB, Heynen AJ, Bear MF. Bidirectional synaptic mechanisms of ocular dominance plasticity in visual cortex. Philos. Trans. R. Soc. Lond. B Biol. Sci. 2009; 364:357–367. [PubMed: 18977732]

12. Fritz J, Shamma S, Elhilali M, Klein D. Rapid task-related plasticity of spectrotemporal receptive fields in primary auditory cortex. Nat Neurosci. 2003; 6:1216–1223. [PubMed: 14583754]
13. Feldman DE, Brecht M. Map plasticity in somatosensory cortex. Science. 2005; 310:810–815. [PubMed: 16272113]
14. Dan Y, Poo MM. Spike timing-dependent plasticity: from synapse to perception. Physiol. Rev. 2006; 86:1033–1048. [PubMed: 16816145]
15. de Villers-Sidani E, Chang EF, Bao S, Merzenich MM. Critical period window for spectral tuning defined in the primary auditory cortex (A1) of the rat. J. Neurosci. 2007; 27:180–189. [PubMed: 17202485]
16. Li Y, Van Hooser SD, Mazurek M, White LE, Fitzpatrick D. Experience with moving visual stimuli drives the early development of cortical direction selectivity. Nature. 2008; 456:952–956. [PubMed: 18946471]
17. Dorrn AL, Yuan K, Barker AJ, Schreiner CE, Froemke RC. Developmental sensory experience balances cortical excitation and inhibition. Nature. 2010; 465:932–936. [PubMed: 20559387]
18. Dahmen JC, Hartley DE, King AJ. Stimulus-timing-dependent plasticity of cortical frequency representation. J. Neurosci. 2008; 28:13629–39. [PubMed: 19074036]
19. Greuel JM, Luhmann HJ, Singer W. Pharmacological induction of use-dependent receptive field modifications in the visual cortex. Science. 1988; 242:74–77. [PubMed: 2902687]
20. Metherate R, Ashe JH. Nucleus basalis stimulation facilitates thalamocortical synaptic transmission in the rat auditory cortex. Synapse. 1993; 14:132–143. [PubMed: 8392756]
21. Bakin JS, Weinberger NM. Induction of a physiological memory in the cerebral cortex by stimulation of the nucleus basalis. Proc. Natl. Acad. Sci. USA. 1996; 93:11219–11224. [PubMed: 8855336]
22. Froemke RC, Merzenich MM, Schreiner CE. A synaptic memory trace for cortical receptive field plasticity. Nature. 2007; 450:425–429. [PubMed: 18004384]
23. Goard M, Dan Y. Basal forebrain activation enhances cortical coding of natural scenes. Nat. Neurosci. 2009; 12:1444–1449. [PubMed: 19801988]
24. Reed A, et al. Cortical map plasticity improves learning but is not necessary for improved performance. Neuron. 2011; 70:121–131. [PubMed: 21482361]
25. Fritz J, Elhilali M, Shamma S. Active listening: task-dependent plasticity of spectrotemporal receptive fields in primary auditory cortex. Hear. Res. 2005; 206:159–176. [PubMed: 16081006]
26. Shuler MG, Bear MF. Reward timing in the primary visual cortex. Science. 2006; 311:1606–1609. [PubMed: 16543459]
27. Martin SJ, Grimwood PD, Morris RGM. Synaptic plasticity and memory: an evaluation of the hypothesis. Annu. Rev. Neurosci. 2000; 23:649–711. [PubMed: 10845078]
28. Hübener M, Bonhoeffer T. Searching for engrams. Neuron. 2010; 67:363–371. [PubMed: 20696375]
29. Brown M, Irvine DR, Park VN. Perceptual learning on an auditory frequency discrimination task by cats: association with changes in primary auditory cortex. Cereb. Cortex. 2004; 14:952–965. [PubMed: 15115736]
30. Edeline J-M, Weinberger NM. Receptive field plasticity in the auditory cortex during frequency discrimination training: selective retuning independent of task difficulty. Behav. Neurosci. 1993; 107:82–103. [PubMed: 8447960]
31. McLin DE 3rd, Miasnikov AA, Weinberger NM. Induction of behavioral associative memory by stimulation of the nucleus basalis. Proc. Natl. Acad. Sci. USA. 2002; 99:4002–4007. [PubMed: 11904444]
32. Han YK, Köver H, Insanally MN, Semerdijan JH, Bao S. Early experience impairs perceptual discrimination. Nat. Neurosci. 2007; 10:1191–1197. [PubMed: 17660815]
33. Abbott LF, Nelson SB. Synaptic plasticity: taming the beast. Nat. Neurosci. 2000; 3:1178–1183. [PubMed: 11127835]
34. Toyoizumi T, Miller KD. Equalization of ocular dominance columns induced by an activity-dependent learning rule and the maturation of inhibition. J. Neurosci. 2009; 29:6514–6525. [PubMed: 19458222]

35. Desai NS, Cudmore RH, Nelson SB, Turrigiano GG. Critical periods for experience-dependent synaptic scaling in visual cortex. Nat. Neurosci. 2002; 5:783–789. [PubMed: 12080341]
36. Royer S, Paré D. Conservation of total synaptic weight through balanced synaptic potentiation and depression. Nature. 2003; 422:518–522. [PubMed: 12673250]
37. Rumsey CC, Abbott LF. Equalization of synaptic efficacy by activity- and timing-dependent synaptic plasticity. J. Neurophysiol. 2004; 91:2273–2280. [PubMed: 14681332]
38. DeWeese MR, Zador AM. Shared and private variability in the auditory cortex. J. Neurophysiol. 2004; 92:1840–1855. [PubMed: 15115790]
39. Lee MG, Hassani OK, Alonso A, Jones BE. Cholinergic basal forebrain neurons burst with theta during waking and paradoxical sleep. J. Neurosci. 2005; 25:4365–4369. [PubMed: 15858062]
40. Hasselmo ME, Sarter M. Modes and models of forebrain cholinergic neuromodulation of cognition. Neuropsychopharmacology. 2011; 36:52–73. [PubMed: 20668433]
41. Zaborszky L, Pang K, Somogyi J, Nadasdy Z, Kallo I. The basal forebrain corticopetal system revisited. Ann N Y Acad Sci. 1999; 877:339–367. [PubMed: 10415658]
42. Lin SC, Nicolelis MA. Neuronal ensemble bursting in the basal forebrain encodes salience irrespective of valence. Neuron. 2008; 59:138–149. [PubMed: 18614035]
43. Fries P, Reynolds JH, Rorie AE, Desimone R. Modulation of oscillatory neuronal synchronization by selective visual attention. Science. 2001; 291:1560–1563. [PubMed: 11222864]
44. Averbeck BB, Latham PE, Pouget A. Neural correlations, population coding and computation. Nat. Rev. Neurosci. 2006; 7:358–366. [PubMed: 16760916]
45. Cohen MR, Maunsell JH. Attention improves performance primarily by reducing interneuronal correlations. Nat. Neurosci. 2009; 12:1594–1600. [PubMed: 19915566]
46. Elhilali M, Fritz JB, Chi TS, Shamma S. Auditory cortical receptive fields: stable entities with plastic abilities. J. Neurosci. 2007; 27:10372–10382. [PubMed: 17898209]
47. Tanner WP, Swets JA. A decision-making theory of visual detection. Psychol. Rev. 1954; 61:401–409. [PubMed: 13215690]
48. Liu RC, Schreiner CE. Auditory cortical detection and discrimination correlates with communicative significance. PLoS Biol. 2007; 5:e173. [PubMed: 17564499]
49. Polley DB, Heiser MA, Blake DT, Schreiner CE, Merzenich MM. Associative learning shapes the neural code for stimulus magnitude in primary auditory cortex. Proc. Natl. Acad. Sci. U.S.A. 2004; 101:16351–16356. [PubMed: 15534214]
50. Wright BA, Sabin AT, Zhang Y, Marrone N, Fitzgerald MB. Enhancing perceptual learning by combining practice with periods of additional sensory stimulation. J. Neurosci. 2010; 30:12868–12877. [PubMed: 20861390]

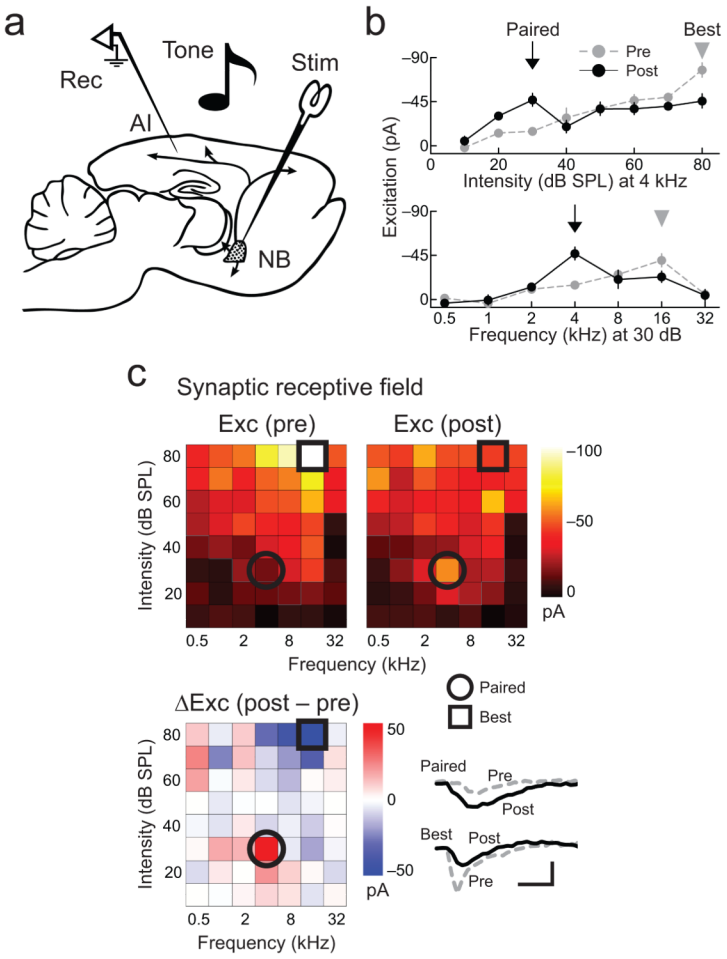

Figure 1.

Example of AI synaptic receptive field modification induced by nucleus basalis pairing. **a**, Experimental preparation. **b**, Example of synaptic tuning curve modification induced by nucleus basalis pairing. Top, intensity sensitivity at 4 kHz. Bottom, frequency tuning at 30 dB SPL. Responses to paired stimulus (30 dB SPL, 4 kHz; arrow) are enhanced while responses to peak level and best frequency (arrowheads) are reduced. **c**, Frequency-intensity synaptic receptive field for same cell in **b**. Top, before (left) and after (right) pairing. Color, EPSC amplitude. Blue lines, threshold. Bottom, change in EPSCs (post-pairing–pre-pairing). Excitation at paired tone (circle) increased from −14.8±3.6 pA to – 46.8±6.6 pA ($p<0.01$, Student's paired two-tailed t-test); excitation at original best stimulus (80 dB SPL, 16 kHz; square) decreased from −98.6±15.4 pA to −43.3±8.1 pA ($p<0.01$). Net excitation across stimuli was similar before and after pairing (before: −1.68 nA, after: −1.51 nA, $p>0.4$). Scale: 50 pA, 40 msec. Error bars show s.e.m.

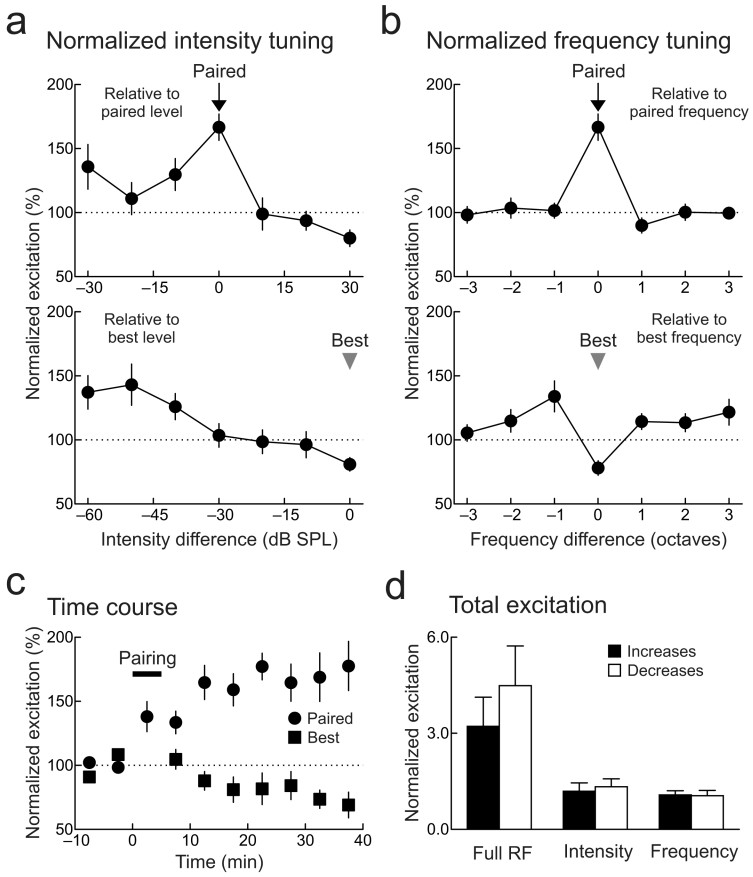

Figure 2.

Conservation of total excitation after pairing.

a, Intensity-specific changes. Top, summary of changes relative to paired level over all recordings (arrow; increase of 66.7%±10.3%, n=29 neurons, $p<10^{-6}$, Student's paired two-tailed t-test). Significant potentiation also occurred to responses evoked by stimuli of the paired frequency and −10 dB lower in intensity (29.7%±12.4%, p<0.04). Bottom, changes to original peak level (arrowhead; decrease of −19.0%±5.2%, $p<10^{-4}$). **b**, Frequency-specific changes. Top, changes relative to paired frequency. Bottom, changes to original best frequency (−21.9%±5.7%, p<0.001). Same recordings as in **a**. **c**, Time course of changes to paired (circles) and original best stimuli (squares). Horizontal bar, pairing. Same recordings as in **a**. **d**, Conservation of total excitation after pairing. Before and after pairing, relative amounts of increases (black) and decreases (white) in synaptic strength were similar across the entire frequency-intensity synaptic receptive field (excitation increased by a factor of 3.2±0.9 and decreased by −4.5±1.2; n=29 neurons, p>0.6, Mann-Whitney), across intensity at paired frequency (increase: 1.2±0.3, decrease:−1.3±0.2; p>0.6), and across frequency at paired intensity (increase: 1.1±0.1, decrease:−1.1±0.2; p>0.5). Same recordings as **a**. Error bars show s.e.m.

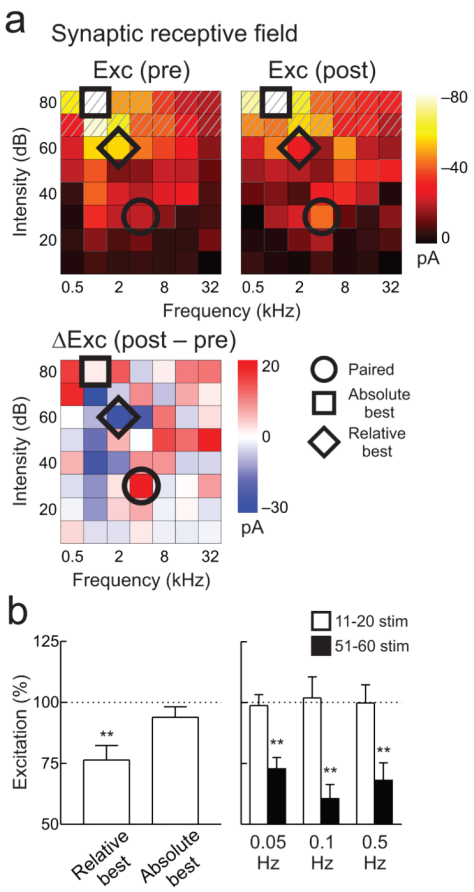

Figure 3.

Best stimuli depression depends on recent sensory experience.

a, Example recording in which for ten minutes post-pairing, no stimuli >60 dB SPL were presented (hatching). Responses to paired tone (30 dB SPL, 4 kHz; circle) increased (before: −21.3 pA, after: −40.7 pA), responses to absolute best stimulus (80 dB SPL, 1 kHz) were unchanged (before: −79.4 pA, after: −81.1 pA; square), responses to 60 dB SPL, 2 kHz tones (relative best stimuli) decreased (before: −54.3 pA, after: −26.0 pA; diamond). **b**, Summary of reduced stimulus set experiments. Left, EPSCs evoked by relative best stimuli depressed (−23.6±5.9%, n=13 neurons, $p<0.006$, Student's paired two-tailed t-test), while absolute best stimuli were unchanged (−6.2±4.3%, $p>0.1$). Right, best stimuli depression was equivalent after 51-60 presentations regardless of rate (black bars; 0.05 Hz: −27.2±4.7%, n=7 neurons, $p<0.002$; 0.1 Hz: −39.5±5.8%, n=5 neurons, $p<0.003$; 0.5 Hz: −31.9±7.2%, n=10 neurons, $p<0.003$; equivalent magnitudes across rates, $p>0.4$, Krusal-Wallis H=1.51). No depression was measurable after 11-20 presentations (open bars). Error bars show s.e.m.

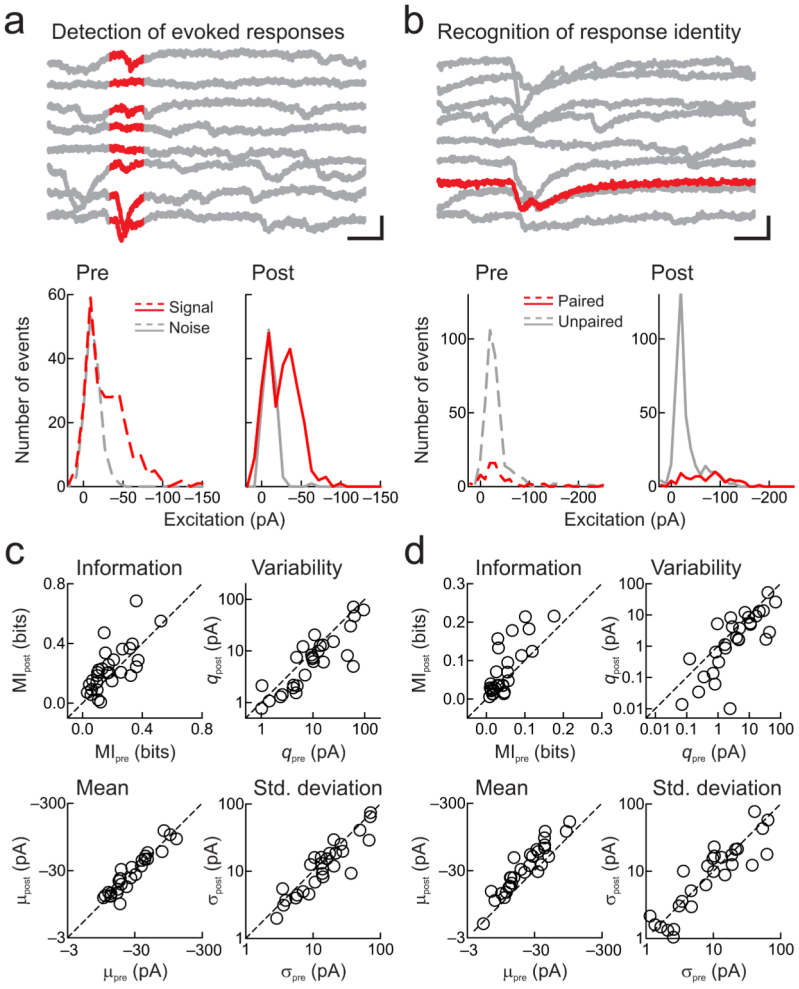

Figure 4.

Pairing decreases synaptic variance to enhance detection and recognition of sensory stimuli. **a**, Example of detection changes. Top, responses to paired frequency (tonal presentation, red). Scale: 40 pA, 60 msec. Bottom, distributions of tone-evoked and spontaneous EPSCs before (left, dashed) and after (right, solid) pairing. Before pairing, signal and noise distributions overlapped (mutual information MI_{pre}: 0.17 bits), and had higher variability q in signal distribution (q_{pre}: 24.8 pA, μ_{pre}: −30.7 pA, σ^2_{pre} : 761.5 pA^2). After pairing, variability decreased and MI increased (MI_{post}: 0.26 bits, q_{post}: 15.1 pA, μ_{post}: −26.2 pA, σ^2_{post} : 396.9 pA^2). **b**, Example of recognition changes. Top, responses evoked by tones of different frequencies (paired tone, red). Scale: 50 pA, 30 msec. Bottom, EPSC distributions for paired (red) and unpaired tones (gray). Initially (left), paired and unpaired responses were similar (MI_{pre}: 0.07 bits, q_{pre}: 69.0 pA, μ_{pre}: −42.2 pA, σ^2_{pre}: 2911.3 pA^2). After pairing, means increased while variability decreased, enhancing MI between paired and unpaired distributions (MI_{post}: 0.18 bits, q_{post}: 25.9 pA, μ_{post}: −72.2 pA, σ^2_{post} : 1871.7 pA^2). **c**, Changes to detection. Top left, MI between signal and noise increased after pairing (before: 0.19±0.02 bits, after: 0.23±0.03 bits, z=−2.0, n=29, p<0.05, two-tailed paired Wilcoxon signed rank test). Top right, q decreased after pairing (before: 19.2±4.6 pA, after: 12.7±3.3 pA, z=2.8, p<0.005). Bottom left, mean amplitudes of signal distributions were unchanged after pairing (before: −33.4±5.3 pA, after: −34.0±5.2 pA, z=−0.7, p>0.5). Bottom right, standard deviations of signal distributions decreased after pairing (before: 24.0±4.8

pA, after: 19.3±3.8 pA, z=2.4, p<0.02). **d**, Changes to recognition. Top left, MI between paired and unpaired stimuli increased (before: 0.05±0.01 bits, after: 0.08±0.01 bits, z=−3.0, p<0.003). Top right, *q* decreased after pairing (before: 11.2±3.1 pA, after: 6.2±2.0 pA, z=2.5, p<0.02). Bottom left, mean amplitudes of paired stimuli responses increased after pairing (before: −27.9±4.2 pA, after: −44.5±6.9 pA, z=−4.4, $p<10^{-4}$). Bottom right, standard deviations of paired stimuli responses were unchanged (before: 15.6±3.2 pA, after: 14.2±3.1 pA, z=0.9, p>0.3).

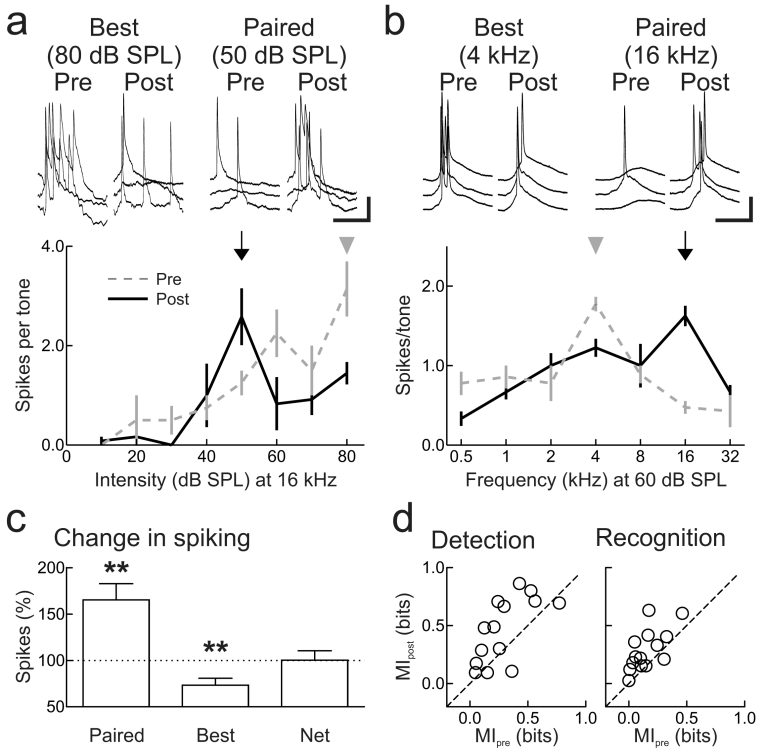

Figure 5.

Nucleus basalis pairing modifies spiking receptive fields.

a, Suprathreshold intensity sensitivity (at 16 kHz) is modified after pairing. Example recording in which responses at paired intensity (50 dB SPL, arrow) increased (before: 1.3±0.3 spikes/tone, after: 2.6±0.6 spikes/tone, $p<0.03$, Student's paired two-tailed t-test), responses at 80 dB SPL (arrowhead) decreased (before: 3.1±0.6 spikes/tone, after: 1.9±0.4 spikes/tone, $p<0.05$). Scale: 5 mV, 50 msec. **b**, Example of changes to suprathreshold frequency tuning (at 60 dB SPL) after pairing (paired frequency 16 kHz, before: 0.5±0.1 spikes/tone, after: 1.6±0.1 spikes/tone, $p<10^{-4}$; best frequency 4 kHz, before: 1.8±0.1 spikes/tone, after: 1.2±0.1 spikes/tone, $p<0.001$). Scale: 20 mV, 25 msec. **c**, Summary of current-clamp recordings. Spiking responses to paired tones increased (65.2±17.6%, n=14 neurons, $p<0.003$), responses to original best stimuli decreased (−26.7±7.4%, $p<0.004$); no net change in spiking (0.2±10.3%, $p>0.9$). **d**, Summary of changes to MI after pairing. Pairing increased MI for detection (before: 0.29±0.06 bits, after: 0.46±0.08 bits, $z=-2.3$, $p<0.02$; left) and recognition (before: 0.16±0.04 bits, after: 0.29±0.05 bits, $z=-2.9$, $p<0.004$; right). Error bars show s.e.m.

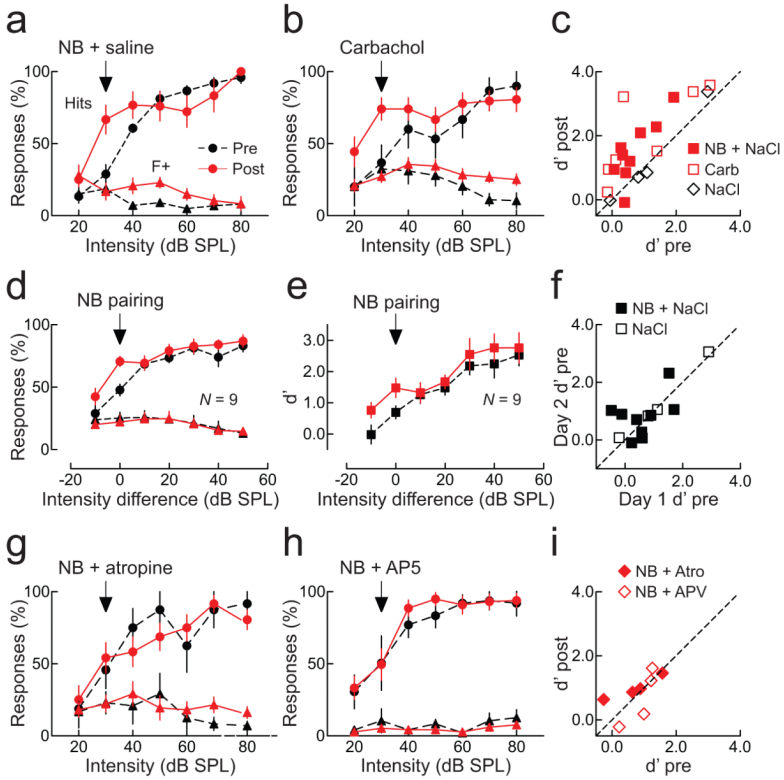

Figure 6.

Nucleus basalis pairing improves auditory detection.

a, Example of enhanced detection after pairing. Hits (circles) at 30 dB SPL increased after pairing (before pairing, black: 28.9±6.6%, after, red: 66.7±10.0%, p<0.005). Responses to foils (triangles) were unchanged (false alarms at 30 dB SPL before, black: 18.7±3.2%, after, red: 16.7±5.7%, p>0.7). d' increased (0.3 to 1.4). **b**, Carbachol pairing enhanced detection without nucleus basalis stimulation. Hits increased (before: 36.7±6.6%, after: 74.1±7.8%, p<0.001), false alarms were unchanged (before: 32.4±7.6%, after: 27.2±4.1%, p>0.5). d' increased (0.1 to 1.3). **c**, Summary of d' values before and after pairing nucleus basalis stimulation with saline (filled squares; d' before: 0.7±0.2, after: 1.5±0.3, N=9 animals, p<0.003), or carbachol pairing without nucleus basalis stimulation (open squares; d' before: 1.0±0.5, after: 2.0±0.5, N=7, p<0.03). Saline pairing without nucleus basalis stimulation had no effect (d' before: 1.2±0.6, after: 1.2±0.7, N=4, p>0.8). **d**, Changes to mean response rate across animals. Response rate increased after pairing at the paired intensity level (hits before pairing: 47.7±4.7%, after: 70.6±4.0%, N=9, p<0.002), and–10 dB SPL from paired level (before: 28.9±6.4%, after: 42.4±6.7%, p<0.03), but not at higher intensities (p>0.1). False alarms were unchanged (before: 25.2±4.6%, after: 22.1±5.5%, p>0.3). **e**, d' for paired stimuli across animals was enhanced after pairing (before: 0.7±0.2, after: 1.5±0.3, p<0.003). **f**, Comparison of detection before pairing on first and second days (d' day one: 0.6±0.2, d' day two: 0.8±0.2, N=9, p>0.4; filled squares) and animals receiving only saline (d' day one: 1.2±0.6, d' day two: 1.3±0.6, N=4, p>0.2; open squares). **g**, Atropine prevented effects of pairing. Hits, false alarms, and d' were unchanged (p>0.6). **h**, AP5 prevented effects of pairing (p>0.5). **i**, Summary of atropine (filled diamonds; d' before: 0.7±0.4, after: 1.0±0.2, N=4, p>0.2) and AP5 (open diamonds; d' before: 0.9±0.2, after: 0.7±0.4, N=4, p>0.4). Error bars show s.e.m.

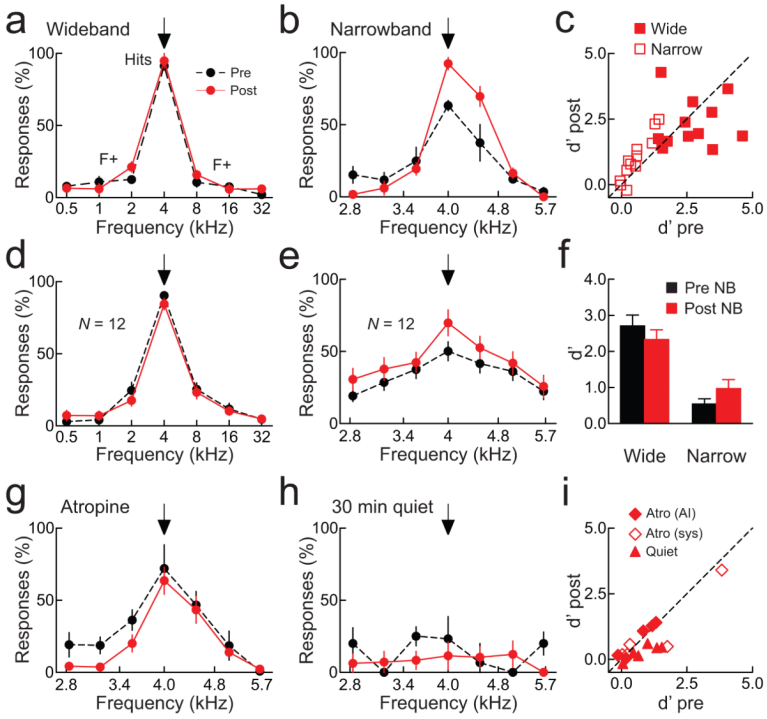

Figure 7.

Nucleus basalis pairing improves recognition.

a, Responses from one animal. Nucleus basalis pairing did not improve 'wideband' performance (d' before: 3.5, after: 2.8). **b**, Responses from another animal. Pairing improved 'narrowband' performance (d' before: 1.3, after: 2.3). **c**, Summary of wideband (filled squares; d' before: 2.7±0.3, after: 2.3±0.3, N=12, p>0.3) and narrowband (open squares; d' before: 0.5±0.1, after: 1.0±0.2, N=12, p<0.005). **d**, Wideband performance was unchanged after pairing (hits before pairing: 90.3±2.8%, after: 84.5±5.0%, N=12, p>0.1). **e**, Narrowband performance was improved after pairing (hits before pairing: 50.1±6.6%, after: 69.9±9.0%, N=12, p<0.005). **f**, d' before (black) and after pairing (red) for wideband (before: 2.7±0.3, after: 2.3±0.3, p>0.3) and narrowband (before: 0.5±0.1, after: 1.0±0.2, p<0.005) tasks. **g**, Atropine infused into AI prevented pairing from improving narrowband behavior (hits before pairing: 72.0±16.4%, after: 63.6±9.5%, p>0.6; false alarms before: 23.4±6.5%, after: 14.6±6.4%, p>0.3; d' before: 1.3, after: 1.4). **h**, When only lower intensity (<50 dB SPL) stimuli were presented 30 minutes post-pairing, narrowband behavior task was unaffected (hits before: 23.3±15.4%, after: 11.5±9.5%, p>0.3; false alarms before: 11.9±4.5%, after: 7.5±1.8%, p>0.3; d' before: 0.4, after: 0.2). **i**, Summary of AI atropine (filled diamonds; d' before: 0.7±0.3, after: 0.8±0.3, N=5, p>0.05), systemic atropine (open diamonds; d' before: 1.2±0.7, after: 1.0±0.6, N=5, p>0.3), or when only quiet stimuli were presented post-pairing (filled triangles; d' before: 0.7±0.2, after: 0.3±0.1, N=6, p>0.05). Error bars show s.e.m.

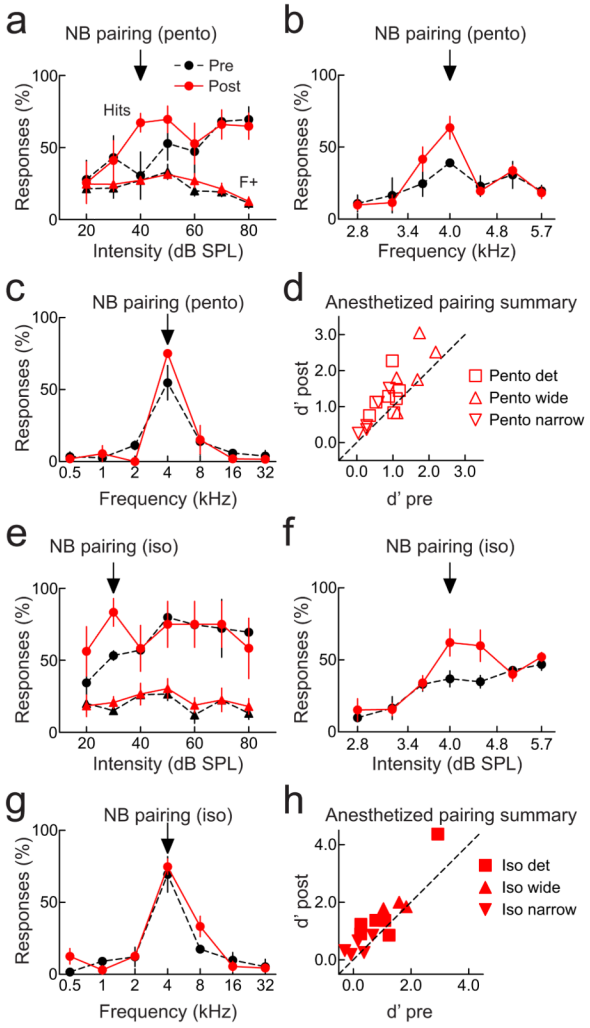

Figure 8.

Pairing under anesthesia improves perception. **a**, Detection; animal anesthetized with pentobarbital during pairing. Hits increased after pairing (before: 30.6±16.3%, after: 67.3±6.5%, p<0.04). False alarms were unchanged after pairing (before: 27.2±5.2%, after: 27.3±1.9%, p>0.4), increasing d' from 0.4 to 0.8. . **b**, Narrowband; pentobarbital anesthesia during pairing. Hits increased (before: 39.0±2.7%, after: 63.5±7.9%, p<0.03), false alarms were unchanged (before: 20.9±2.9%, after: 22.4±3.5%, p>0.7), increasing d' from 0.6 to 1.1. **c**, Wideband; pentobarbital anesthesia during pairing (hits before: 54.8±11.9%, after: 75.1±1.1%, p>0.1; false alarms before: 6.8±1.7%, after: 4.3±2.0%, p>0.3; d' before: 1.7, after: 1.8). **d**, Summary of experiments with pentobarbital anesthesia during and 1-3 hours post-pairing. Performance on wideband (triangles), narrowband (inverted triangles), and detection (squares) tasks was assessed 30-60 minutes pre-pairing and 1-2 hours after recovery. Performance improved on detection (d' before: 0.9±0.1, after: 1.3±0.2, N=7, p<0.03) and narrowband recognition (d' before: 0.4±0.1, after: 0.7±0.2, N=5, p<0.02), but not wideband (d' before: 1.6±0.2, after: 2.0±0.4, N=5, p>0.05). **e**, Detection; animal anesthetized with isoflurane before pairing. Hits increased after pairing (before: 53.3±3.3%, after: 83.3±9.6%, p<0.03). False alarms were unchanged (before: 15.1±2.6%, after: 20.7±4.0%, p>0.1), increasing d' from 0.8 to 1.4. **f**, Narrowband recognition; animal anesthetized with isoflurane during pairing. Hits increased (before: 36.8±5.5%, after:

62.1±9.4%, p<0.04), false alarms were unchanged (before: 30.6±3.6%, after: 36.1±4.2%, p>0.1), increasing d' from 0.2 to 0.7. **g**, Wideband recognition; animal anesthetized with isoflurane during pairing. Behavior was unchanged (hits before: 69.4±12.3%, after: 74.7±5.4%, p>0.7; false alarms before: 9.2±1.9%, after: 11.9±2.2%, p>0.3; d' before pairing: 1.8, after: 1.8). **h**, Summary of experiments with isoflurane anesthesia during pairing. Performance improved on detection (d' before: 1.1±0.4, after: 1.7±0.5, N=6, p<0.04) and narrowband (d' before: 0.2±0.2, after: 0.5±0.1, N=5, p<0.05), but not wideband (d' before: 1.5±0.2, after: 1.9±0.1, N=3, p>0.1). Error bars show s.e.m.